Journal of
Materials Chemistry C

Supporting Information

Evolution of $CaGd_2ZnO_5:Eu^{3+}$ nanostructures for rapid visualization of latent fingerprints†

G. Seeta Rama Raju,[a] Jin Young Park,[b] Ganji Purnachandra Nagaraju,[c] E. Pavitra,[a] Hyun Kyoung Yang,[b] Byung Kee Moon,[a] Jae Su Yu,[d,] Yun Suk Huh,[e,]* and Jung Hyun Jeong,[a,]**

[a]*Department of Physics, Pukyong National University, Busan-48513, Republic of Korea*

[b]*Department of LED convergence Engineering, Pukyong National University, Busan-48573, Republic of Korea*

[c]*Department of Hematology and Medical Oncology, Winship Cancer Institute, Emory University, Atlanta, GA – 30322, USA*

[d]*Department of Electronic Engineering, Institute for Wearable Convergence Electronics, Kyung Hee University, 1 Seocheon-dong, Giheung-gu, Yongin-si, Gyeonggi-do 446-701, Republic of Korea*

[e]*Department of Biological Engineering, Biohybrid Systems Research Center (BSRC), Inha University, Incheon, 402-751, Republic of Korea*

**Email:*

jsyu@khu.ac.kr (Prof. J. S. Yu)

yunsuk.huh@inha.ac.kr (Prof. Y. S. Huh)

jhjeong@pknu.ac.kr (Prof. J. H. Jeong)

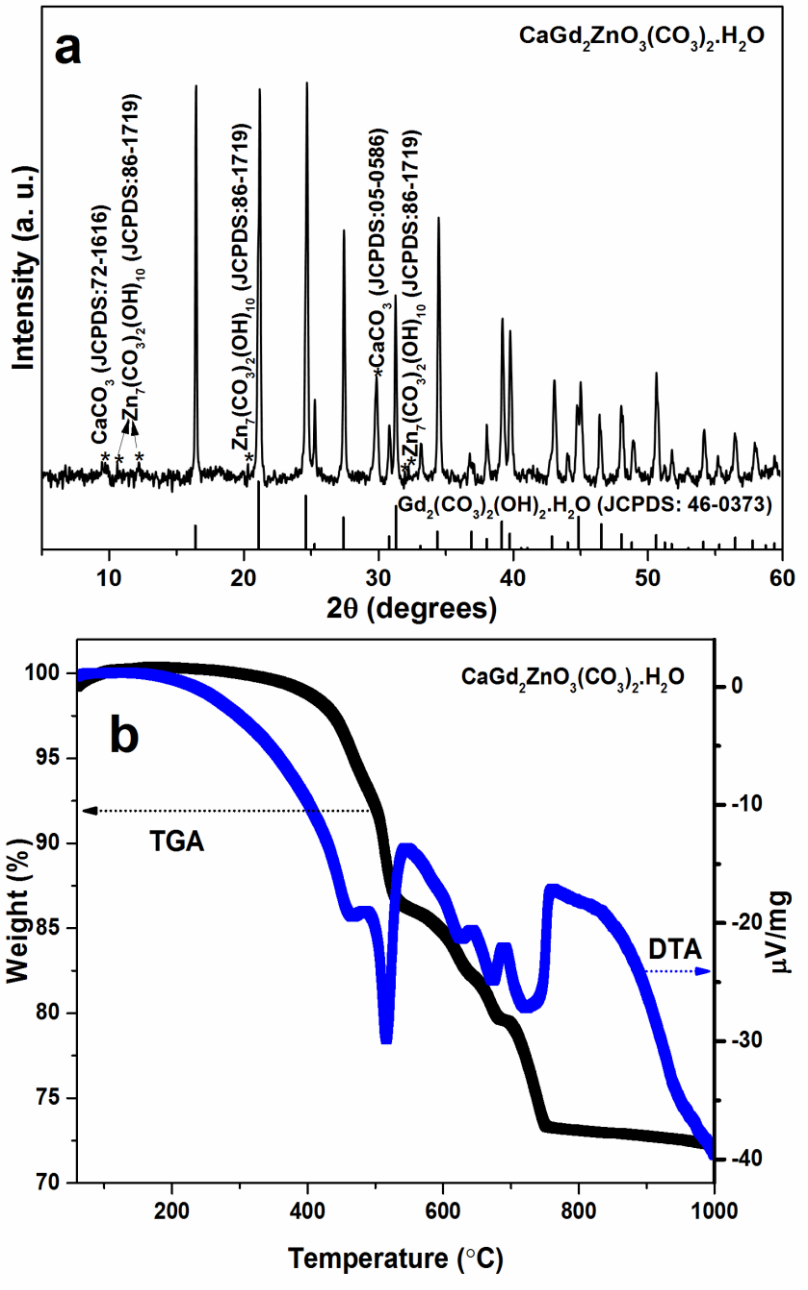

Fig. S1 (a) XRD pattern of CGZOCH nanorod bundles and (b) TG/DTA curves of CGZOCH nanorod bundles

Figure S1(b) shows the TG/DTA curves of CGZOCH precursor sample. The TGA curve displayed that CGZOCH began to decompose at 440 °C and exhibited a total weight loss of 27%. The weight loss was observed in four phases up to 750 °C and then no considerable weight loss was recorded. The corresponding DTA curve displayed endothermic peaks related

to the weight loss and phase transformation. Initially, minimum amount of (2.3 wt%) weight loss was observed up to 440 °C due to the simultaneous dehydration and the decomposition of organic residuals such as carbonates.[1] The corresponding small endothermic DTA peak was related to the physically absorbed water on the surface of the particles. The second major weight loss was observed (about 11 wt%) when the temperature reached up to 540 °C, which was related to the removal of remaining hydroxyl groups due to the dehydration of hydrated compounds and the self-condensation of oxycarbonates. The DTA curve shows the sharp endothermic peak at 520 °C, which is related to phase transformation from carbonate to oxide form. The third (11 %) and fourth (6 %) weight loss phases were observed when the temperatures increased to 700 and 750 °C, respectively as a result of the complete disappearance of the characteristic bands of H_2O and CO_3^{2-} due to the release of OH and CO_2 molecules, respectively. The corresponding DTA peaks at 626 and 670 °C confirmed the removal of organic species, however the broader exothermic peaks with the band maximum at 760 °C might indicate the starting of Ostawlad's ripening process.

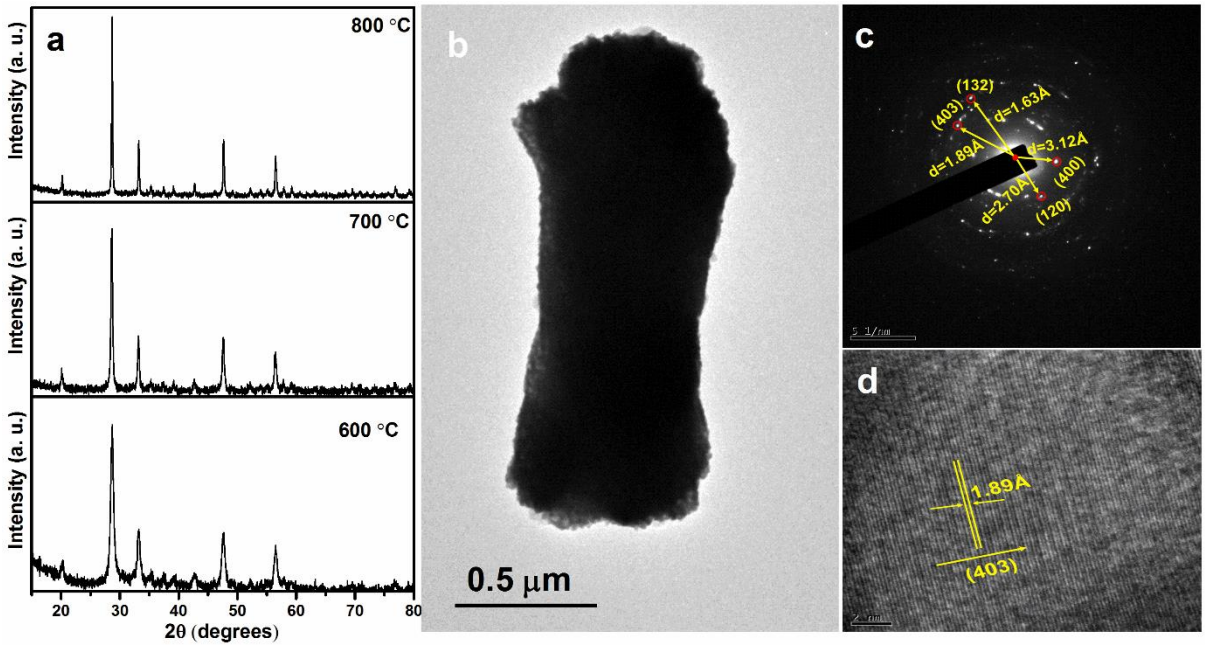

Fig. S2 (a) XRD patterns as a function of calcination temperature of CGZO nanorod bundles (b) TEM image of the CGZO nanorod bundle after calcination at 700 °C (c) corresponding SAED pattern (d) corresponding HR-TEM image

Figs.S2 (b)-(d) show the TEM and corresponding SAED and HR-TEM patterns after calcination at 700 °C. TEM image shows porous nature of the nanorod bundle, as shown in Figure S2(b). The SAED pattern exhibited the discontinuous ring patterns with sharp spots (Figure S2(c)), indicating the existence of ultra-thin nanoparticles in the CGZO nanorod bundles.[2] The bright spots in the ring pattern correlate with the XRD patterns. The HRTEM image clearly shows the lattice fringes with interplanar spacing of 1.89Å corresponding to (403) the plane (Figure S2(d).

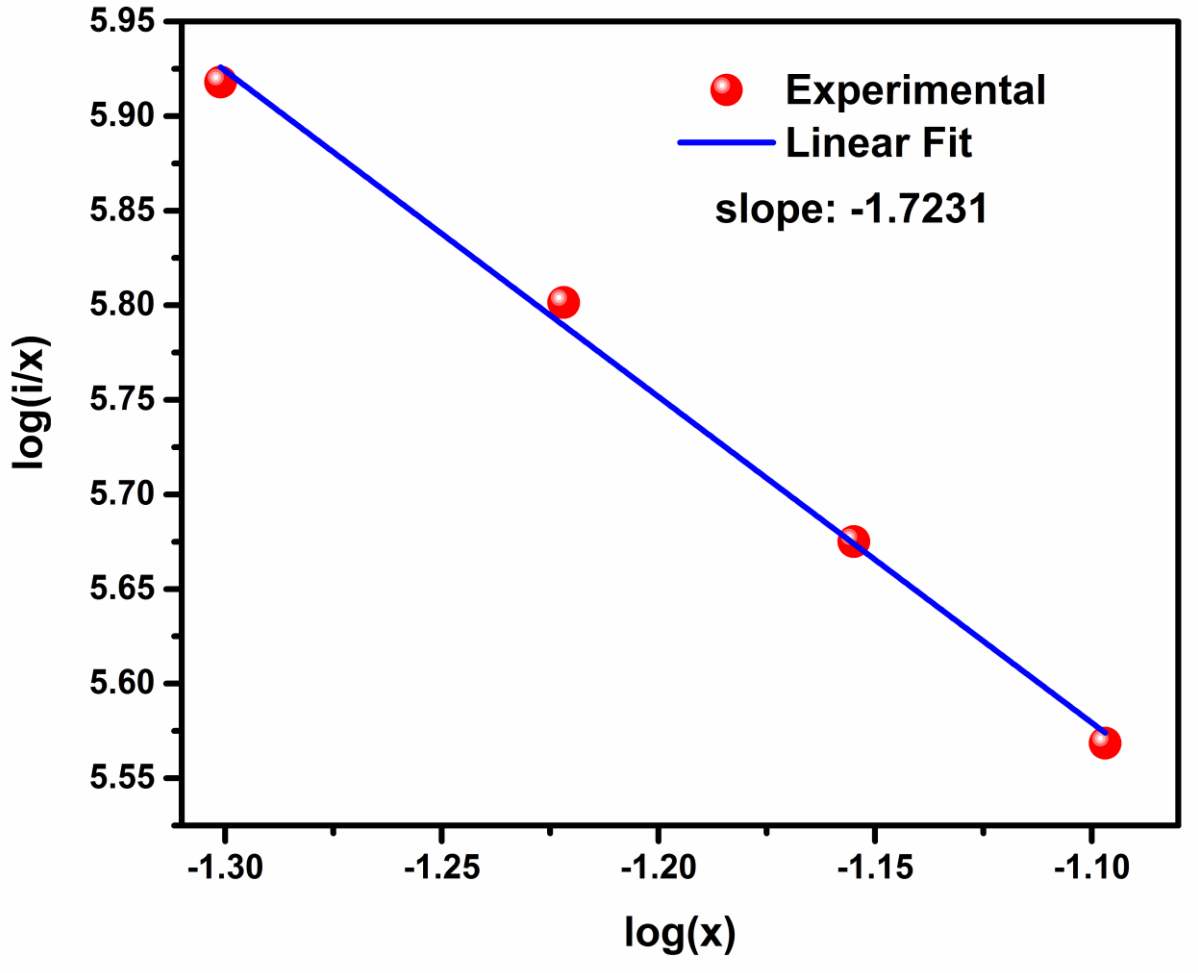

Fig. S3 Relationship plot between log(x) and log (i/x) for $^5D_0 \rightarrow {}^7F_2$ transition under 254 nm excitation.

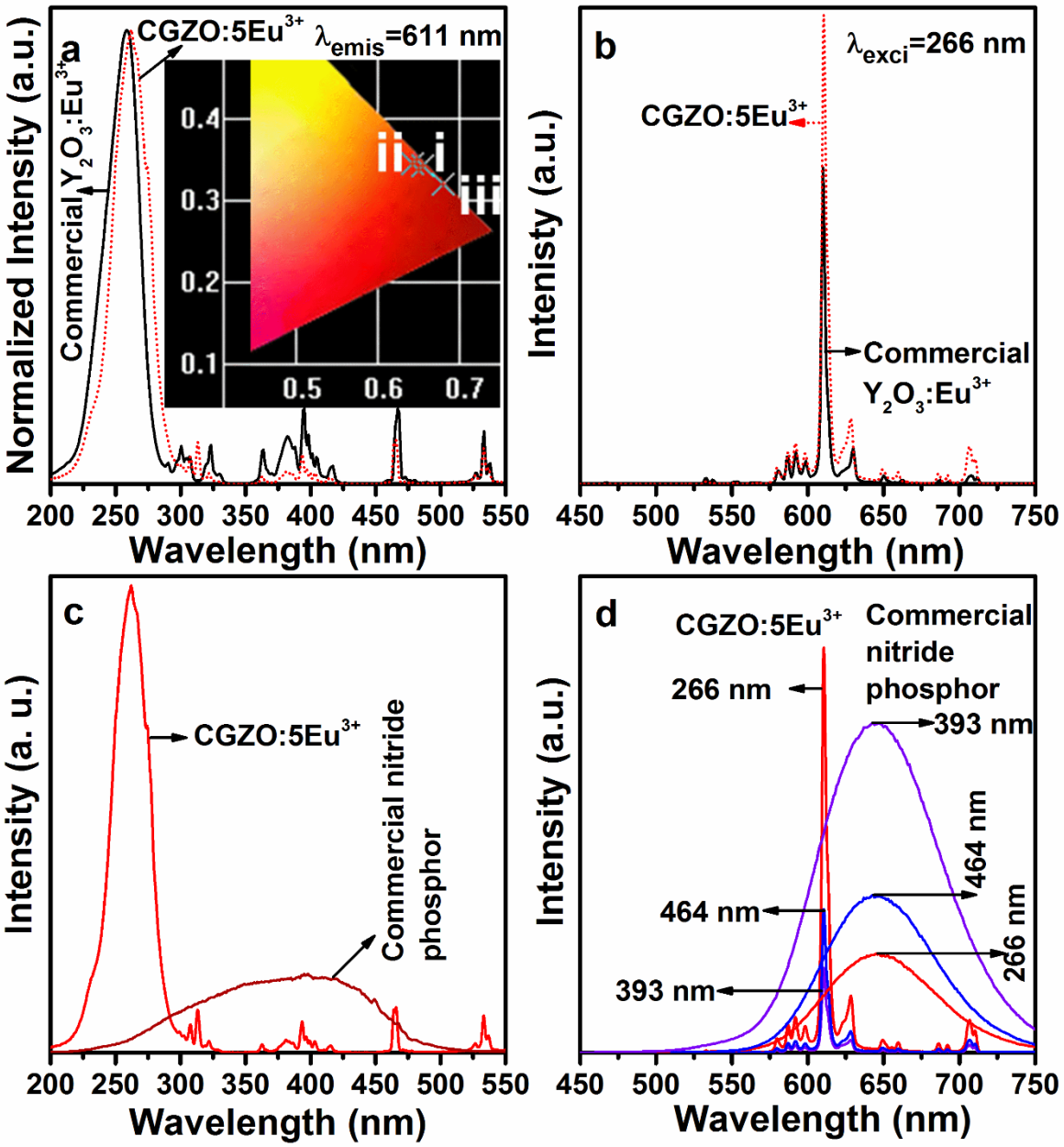

Fig. S4 PLE and PL intensities comparison between the commercially available red phosphors and CGZO:5Eu^{3+} nanorod bundles (a) (b) PLE and PL comparison between commercially available Y_2O_3:Eu^{3+} and CGZO:5Eu^{3+} nanorod bundles (c) (d) PLE and PL comparison between commercial $Sr_2Si_7Al_3ON_{13}$:Eu^{2+} and CGZO:5Eu^{3+} nanorod bundles.

To clarify the red emission richness, the CGZO: 5Eu^{3+} nanorod bundles were compared with the commercially available Y_2O_3: Eu^{3+} (Nichia, Japan) and $Sr_2Si_7Al_3ON_{13}$:Eu^{2+} (Yantai shield, China) red phosphors, as shown in Figure S4. Figs. S4 (a) and S4(c), show the excitation

spectra comparison between the commercial phosphors and CGZO:5Eu^{3+} nanorod bundles. strong UV excitation was observed for CGZO:5Eu^{3+} nanorod bundles as compared to the commercial Y_2O_3:Eu^{3+} phosphor, however, for understanding the position of CTB maxima, the excitation intensities were normalized. CTB was placed in the lower energy region as compared to the Y_2O_3:Eu^{3+} phosphor, which is a good sign because it facilitates the energy transfer from lowest strong absorption band to the hypersensitive transitions of the Eu^{3+} ions. Also, the full width at half maximum (FWHM) is relatively broader (FWHM=35.32) as compared to that of commercial Y_2O_3:Eu^{3+} (FWHM= 33.39) red phosphor, indicating that the CGZO:5Eu^{3+} have intense and broader UV excitation region to excite the Eu^{3+} ions with high-energy as compared to Y_2O_3:Eu^{3+} phosphors. All of the above mentioned features induces 1.47 times higher-intense red emission from CGZO:5Eu^{3+} nanorod bundles with the CIE coordinates (0.656, 0.342) than that of commercial Y_2O_3:Eu^{3+} phosphor with the chromaticity coordinates (0.642, 0.344) (Figure S4(b) and inset of Fig S4(a)). Clearly, from the chromaticity coordinates and CIE diagram, CGZO:5Eu^{3+} exhibits high-color purity than that of Y_2O_3:Eu^{3+} commercial phosphor. On the other hand, when compared with the $Sr_2Si_7Al_3ON_{13}$:Eu^{2+} red phosphor, CGZO:5Eu^{3+} nanorod bundles exhibited less area in the NVU and visible excitation region, as shown in Figure S4 (c). However, the excitation intensity of CGZO:5Eu^{3+} nanorod bundles in the UV region is very strong and almost similar at blue ($^7F_0 \rightarrow {}^5D_2$) transition region as compared to that of $Sr_2Si_7Al_3ON_{13}$:Eu^{2+} phosphors. Under UV excitation, the emission intensity of CGZO:5Eu^{3+} is 4 times higher than that of $Sr_2Si_7Al_3ON_{13}$:Eu^{2+} phosphor (Figure S4(d)). While, both emission intensities are almost similar under visible excitation, the commercial phosphor appears in the deep red region with the CIE coordinates (0.681, 0.319) (Figure S5(a)), indicating that CGZO:5Eu^{3+} nanorod bundles are better red compensators for getting the natural white-light emission when mixing with yellow or green phosphors under visible

excitation. Thus, these results indicate that CGZO:5Eu^{3+} nanorod bundles are cost-effective alternative red emission source, which can be replaced for the commercially available expensive nitride and Y_2O_3:Eu^{3+} red phosphors.

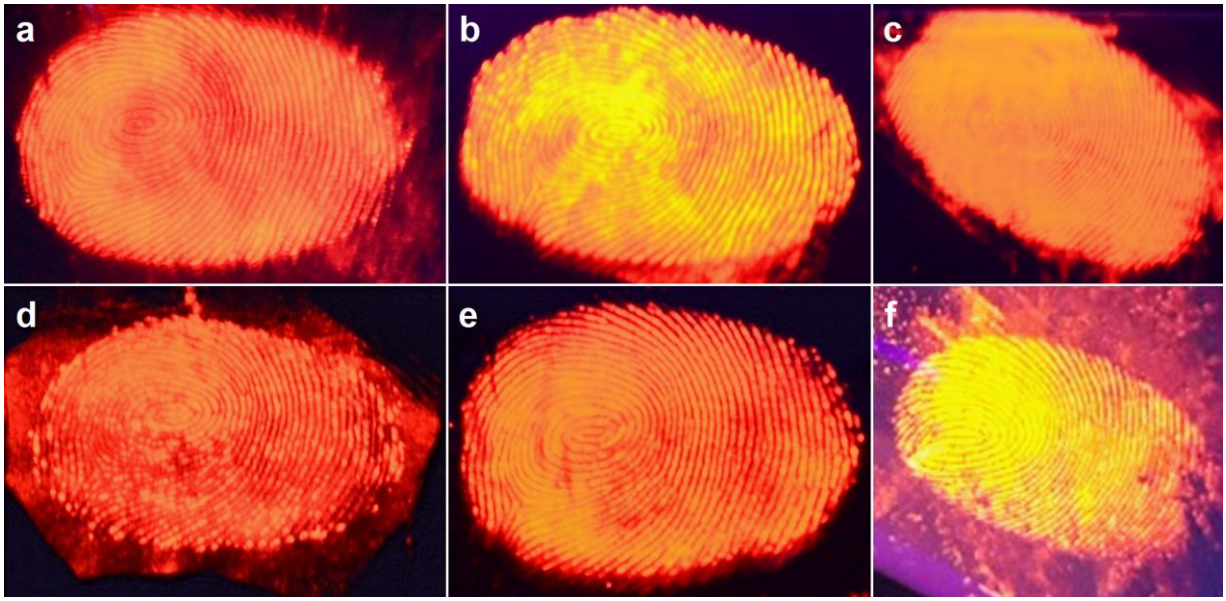

Fig. S5 Digital photographs under 254 nm UV excitation of the CGZO:5Eu^{3+} nanorod bundle stained latent fingerprints from various substrate surfaces: (a) CD, (b) stainless steel, (c) credit card, (d) SLS glass, (e) aluminum foil, and (f) plastic.

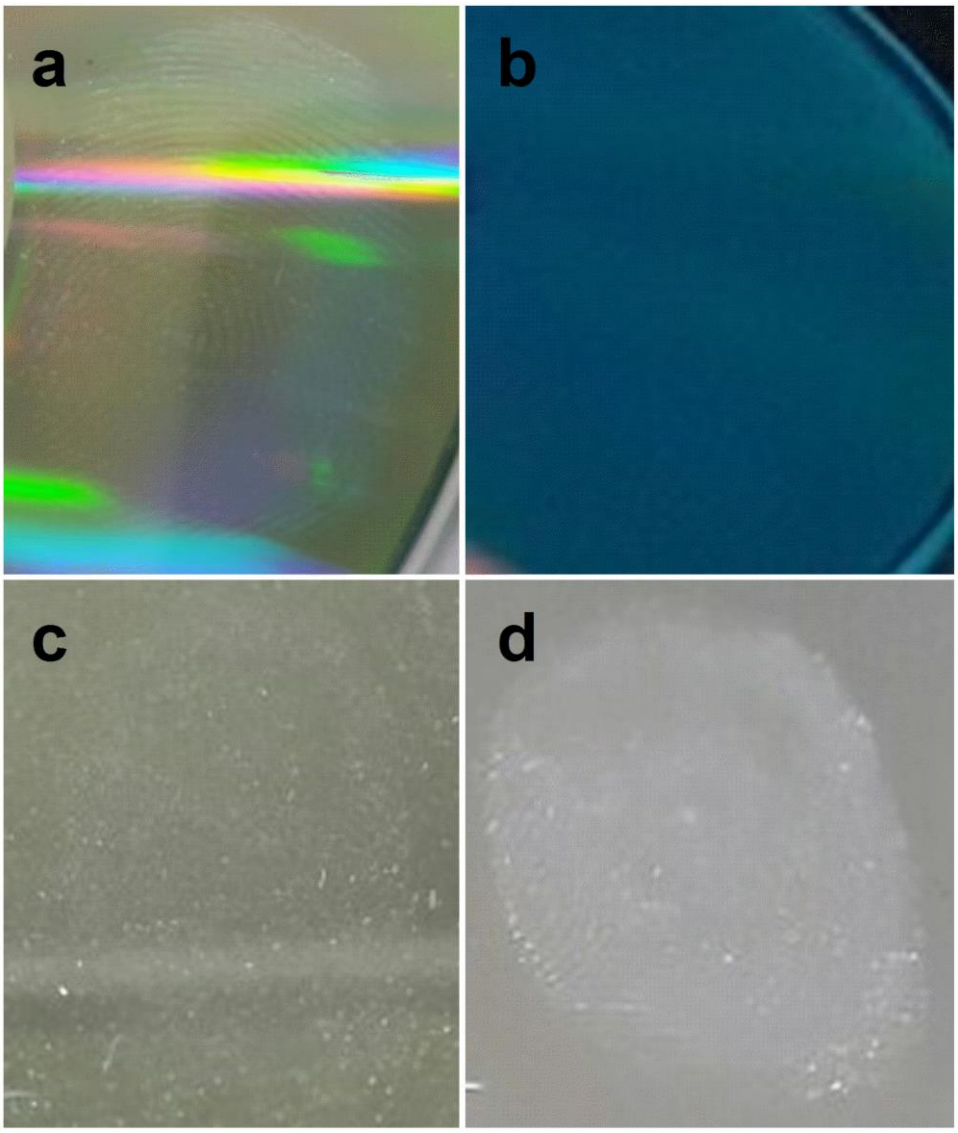

Fig. S6 Digital photographs without CGZO:5Eu^{3+} nanorod bundles stained latent fingerprints deposited CD surface (a) bare fingerprint and (b) under 254 nm UV excitation, and SLS glass substrate (c) bare fingerprint, and (f) under 254 nm UV excitation .

According to the literature, the autofluorescence between 300 and 400 nm is possible when exciting with 254 nm UV-radiation, and it requires specialist UV sensitive devices. The autofluorescence depends on many factors such as deposition time (morning or after lunch) and aging etc.[3] In the present work, without staining the CGZO:5Eu^{3+} nanorod bundles, we have examined the autofluorescence from the trypotophon-containing proteins of fresh fingerprints deposited CD and SLS glass substrates Fig. S6(a) and Fig. S6(c). However, when exciting with 254 nm UV-radiation, no fluorescence was observed from the fingerprints deposited on the CD surface due to the dominating background interference of CD (Fig. S6(b)) and very weak autofluorescence was observed from the fingerprints deposited on the SLS glass substrate (Fig. S6(d)), indicating that the autofluorescence didn't show any effect on the

luminescence of CGZO:5Eu^{3+} nanorod bundles and these bundles inhibit the background interference and provides excellent visualization of latent fingerprints.

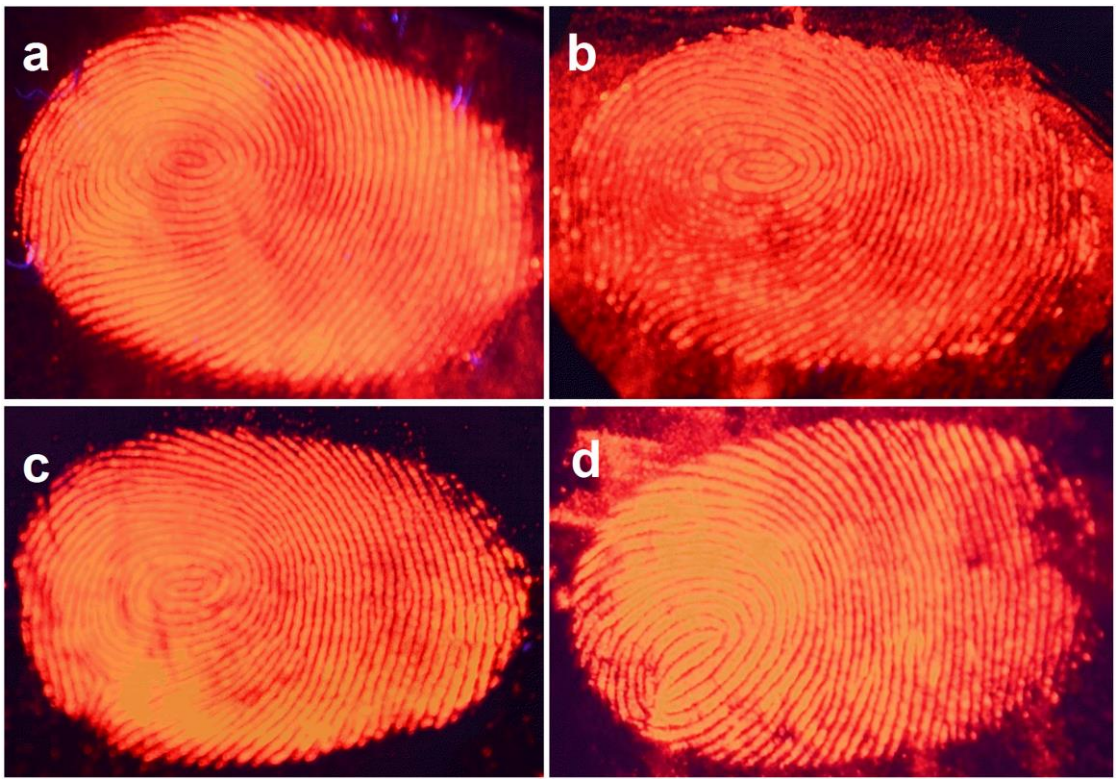

Fig. S7 Digital photographs under 254 nm UV excitation displayed the CGZO:5Eu^{3+} nanorod bundles stained latent fingerprints after aging for 5 days on various substrate surfaces: (a) CD, (b) SLS glass, (c) aluminum foil, and (d) plastic.

1. I. Y. Park, D. Kim, J. Lee, S. H. Lee, K.-J. Kim, *Mat. Chem. Phys.* **2007**, *106*, 149-157.
2. F. Ozel, E. Aslan, B. Istanbullu, O. Akay, I. Hatay Patir, *Appl. Catal., B* **2016**, *198*, 67-73.
3. S. A. G. Lambrechts, A. van Dam, J. de Vos, A. van Weert, T. Sijen, M. C. G. Aalders, *Forensic Sci. Int.* **2012**, *222*, 89-93.